Effect of laser-induced antidiffusion on excited conduction electron dynamics in bulk semiconductors

T. Apostolova,[1] D. H. Huang,[1] P. M. Alsing,[2,3] J. McIver,[3] and D. A. Cardimona[1]
[1]*Air Force Research Lab (AFRL/VSSS), Kirtland Air Force Base, New Mexico 87117*
[2]*The Albuquerque High Performance Computing Center, University of New Mexico, Albuquerque, New Mexico 87131*
[3]*Department of Physics and Astronomy, University of New Mexico, Albuquerque, New Mexico 87131*
(Received 9 April 2002; published 26 August 2002)

By including the effect of local fluctuations in the electron kinetic energies, the kinetic Fokker-Planck-type equation for excited conduction electrons in bulk semiconductors (such as GaAs, Si, etc.) is systematically derived in the presence of a pulsed laser beyond the classical limit. A new contribution from an antidiffusion process is found as a correction to the spontaneous-phonon emission from drifting electrons in addition to contributions from joule heating and a field-dependent diffusion of electrons. The stimulated interband optical transitions of electrons from single-photon absorption are included as one of the source terms of the equation. Some possible types of damage in semiconductors including optical, electrical, and structural damage are explored. The calculated results demonstrate the existence of a kinklike feature in the electron distribution function around the edge of the conduction band due to antidiffusion. The energy spectra of the electron distribution function are studied at different times and used to analyze the transient behavior of both the conduction electron density and the hot-electron temperature.

DOI: 10.1103/PhysRevB.66.075208 PACS number(s): 61.82.Fk, 79.20.Ap, 79.20.Fv

I. INTRODUCTION

Optical and transport properties of semiconductors determine their applications as optoelectronic devices. These properties are found to be altered when semiconductor devices are exposed to an intense laser field due to the creation of a large number of free conduction electrons. Therefore, it is of great importance to describe the microscopic processes taking place when a semiconductor is irradiated by an intense laser. The critical electron density sufficient to damage the crystal is defined as the one at which the laser is completely reflected by the induced free-electron plasma.[1] One of the mechanisms for electron production in the conduction band (CB) is through collisional ionization of valence electrons by conduction electrons with kinetic energy larger than the band gap (E_G). In order to reach this threshold energy for collisional ionization, the conduction electrons have to gain energy from the incident laser field.

The first fact which was recognized[2,3] is that an electron in the CB of a dielectric can continuously gain or lose energy through interaction with phonons and the incident laser field. In this picture, the energy change of electrons is small if the laser field is not extremely strong, and the electron energy displacements are random with time. This is reminiscent of Brownian motion of electrons in energy space. By assuming a Brownian motion for conduction electrons in energy space, Uhlenbeck and Ornstein[4] proposed a phenomenological equation and applied it to the time evolution of the electron distribution function, where an assumption that electron energy does not change significantly over many collisions is introduced. The coefficients of this kinetic equation were obtained under the relaxation-time approximation which can be explicitly calculated for the scattering of electrons with optical and acoustic phonons.[5,6]

It is well known that free carriers cannot directly absorb the incident laser field without assistance from defects (impurities and phonons) (Ref. 7) since $\mathbf{A}(t)\cdot\langle u_B^c(\mathbf{r})|\hat{\mathbf{p}}|u_B^c(\mathbf{r})\rangle = 0$ in the dipole approximation, where $\mathbf{A}(t)$ is the vector potential for a spatially uniform laser field and $u_B^c(\mathbf{r})$ is the Bloch function for conduction electrons. This is a direct result of the impossibility of conserving energy and momentum simultaneously during the absorption of a photon by an electron. Several groups[8–10] have derived a quantum kinetic equation for calculating the electron distribution function in the conduction band based on a method involving an equation of motion with a Hamiltonian consisting of an electron-phonon interaction and a canonical momentum in the presence of a laser field. This formalism reduced to a Fokker-Planck-type kinetic equation[11,12] under the physical conditions that the change of electron energy is small in the CB and that the photon energy of the laser is smaller than E_G. However, both the classical joule heating effect from power dissipation of the laser field within the material and the field-dependent diffusion of conduction electrons in energy space were neglected in this previous work, although a quantum correction to the electron-phonon coupling ($\propto|C_q|^2$ and referred to as phonon-assisted free-carrier absorption) from the laser field was included. This correction term becomes important only when the laser field is very strong and either the lattice temperature is very high or the electron initial kinetic energy is very large. More recently, a numerical approach based on Boltzmann equations for both electron and phonon occupation probabilities with proper collision integrals[13] was used to find the time dependence of electron and phonon occupations. Joule heating and field-induced diffusion were still missing in this approach, although the modifications to the electron-phonon ($\propto|C_q|^2$) and even the Coulomb [$\propto|V_C(q)|^2$] interactions due to an incident laser field were taken into account.

In the present work, we first note that the conduction elec-

trons in semiconductors cannot directly absorb the incident laser field without assistance from defects.[7] Under the condition that $\Omega_L \tau \ll 1$, where Ω_L and τ are the laser-field frequency and carrier relaxation time in semiconductors, respectively, the electrons acquire a certain momentum over time in the presence of the laser field. However, the electrons will acquire an average power from the laser field under the condition of $\Omega_L \tau \gg 1$, which produces a local fluctuation in the electron kinetic energies or a drift of conduction electrons in energy space towards higher energies, as can be seen from a shifted Fermi-Dirac model.[14] We further find that joule heating of conduction electrons can be the main energy-gain mechanism to reach the threshold energy for impact ionization, and both joule heating and field-dependent diffusion of conduction electrons can be derived simultaneously from the energy-drift effect instead of inserting them into the equation phenomenologically.[2–4] More importantly, we have uncovered an antidiffusion process due to the correction to a spontaneous-phonon emission from drifting conduction electrons. Some of the preliminary results of the current research (thermal diffusion and temperature-dependent band-gap effects) have been presented elsewhere.[15] However, in this paper we mainly concentrate on the effects of the laser pulse profile (frequency detuning, peak intensity, and pulse duration) on the dynamics of excited conduction electrons and present new numerical results associated with these effects. Compared with our previous paper,[15] we have presented the detailed quantum-mechanical derivation of the Fokker-Planck-type equation and additionally included the Auger recombination process due to the Coulomb interaction between electrons and holes, which has a huge effect on the population of electrons around the edge of the conduction band.

The question we ask is, are there any new effects arising from the electron energy drift besides joule heating and field-dependent diffusion? We have found the answer to this question to be yes. In this paper, based on Fermi's golden rule we derive a dynamical equation for conduction electrons in semiconductors in the presence of a laser field. This equation reduces to the quantum kinetic equation[11] in the absence of a laser field. By including the energy-drift effect in the presence of the laser field, however, we find a new antidiffusion process for conduction electrons as a correction to the spontaneous-phonon emission from drifting electrons. The source terms in this equation are calculated simultaneously up to second order in perturbation theory. We also discuss some possible types of damage in semiconductors including optical, electrical, and structural damage. We find a kinklike feature around the edge of the conduction band in the energy spectra of the electron distribution function due to the existence of the antidiffusion process. We also analyze the transient behavior of both the conduction electron density and the hot-electron temperature.

The organization of this paper is as follows. In Sec. II, we present our scattering model within Fermi's golden rule. The dynamical equation in the absence of a laser field is derived in Sec. III. The effect of the energy drift of conduction electrons in the presence of a laser field is taken into account in Sec. IV. A discussion of stimulated interband electron transitions and the analytical expressions for all the other source terms up to second order in perturbation theory are presented in Sec. V. This section also includes a discussion of some possible types of damage in semiconductors. Numerical results for the effects of antidiffusion on the electron distribution function are presented in Sec. VI, along with the transient properties of the electron density and average kinetic energy (hot-electron temperature). The paper is concluded in Sec. VII with some remarks.

II. SCATTERING MODEL

Let us start by considering a laser incident on an undoped bulk semiconductor material [e.g., GaAs(polar), Si(nonpolar)] at finite lattice temperature T and with temperature-dependent E_G separating the conduction and valence bands. Because of finite lattice temperatures, there exist electron-phonon interactions in this system, including electron scattering with optical and acoustic phonons. At the same time, there exists a drift of conduction electrons in energy space due to local fluctuations in the electron kinetic energies (different from phonon-assisted free-carrier absorption of photons), stimulated interband optical transitions due to single-photon excitation, impact ionization, and Auger recombination due to the Coulomb interaction between electrons and holes.

The total Hamiltonian of the interacting electron-phonon system exposed to a laser field in the second quantization can be written as

$$\hat{\mathcal{H}}(t) = \hat{\mathcal{H}}_0(t) + \hat{\mathcal{H}}_I(t), \tag{1}$$

where the noninteracting part of the Hamiltonian is given by

$$\hat{\mathcal{H}}_0(t) = \sum_{\mathbf{k}} E_k^e \hat{a}_{\mathbf{k}}^\dagger(t)\hat{a}_{\mathbf{k}}(t) + \sum_{\mathbf{q}} \hbar\omega_q \hat{b}_{\mathbf{q}}^\dagger(t)\hat{b}_{\mathbf{q}}(t) \tag{2}$$

and the interacting part takes the form of[8,16]

$$\hat{\mathcal{H}}_I(t) = \sum_{\mathbf{k},\mathbf{q}} C_{\mathbf{q}} \hat{a}_{\mathbf{k}+\mathbf{q}}^\dagger(t)\hat{a}_{\mathbf{k}}(t)[\hat{b}_{\mathbf{q}}(t) + \hat{b}_{-\mathbf{q}}^\dagger(t)] + \sum_{\mathbf{k}} [F_{\mathbf{k}} \hat{a}_{\mathbf{k}}^\dagger(t)\hat{d}_{-\mathbf{k}}^\dagger(t) + F_{\mathbf{k}}^* \hat{d}_{-\mathbf{k}}(t)\hat{a}_{\mathbf{k}}(t)]. \tag{3}$$

Here, the laser field is treated classically with $F_{\mathbf{k}}$ being the interband dipole-coupling coefficient between the laser field and electrons.[16] $\hat{a}_{\mathbf{k}}^\dagger(t)$ [$\hat{d}_{\mathbf{k}}^\dagger(t)$] and $\hat{a}_{\mathbf{k}}(t)$ [$\hat{d}_{\mathbf{k}}(t)$] are the electron [hole] creation and annihilation operators satisfying Fermi-Dirac statistics, while $\hat{b}_{\mathbf{q}}^\dagger(t)$ and $\hat{b}_{\mathbf{q}}(t)$ stand for the phonon creation and annihilation operators obeying Bose-Einstein statistics. $E_k^e = \hbar^2 k^2 / 2m_e^*$ is the free-electron kinetic energy in the conduction band with effective mass m_e^*, $\hbar\omega_q$ is the phonon energy, and $C_{\mathbf{q}}$ is the electron-phonon coupling coefficient.[8] The exchange energy which changes the electron energy dispersion[17] can be neglected (much smaller than E_F) under the condition of $4/(3\pi a_B^*) \ll (2n_{3D}^e)^{1/3}$ due to the strong screening at high electron densities, where $a_B^* = 4\pi\epsilon_0\epsilon_r\hbar^2/m_e^* e^2$ is the effective Bohr radius, n_{3D}^e is the

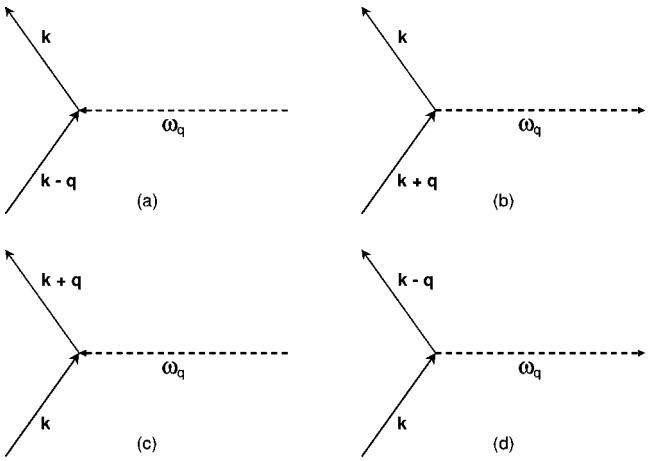

FIG. 1. Diagrams for electron scattering into state $|\mathbf{k}\rangle$ in (a) (with phonon absorption) and (b) (with phonon emission) and for electron scattering out of state $|\mathbf{k}\rangle$ in (c) (with phonon emission) and (d) (with phonon absorption). Here, the upward solid arrows represent the electron states with the wave vector indicated. The horizontal dashed arrows stand for the phonon states with the phonon frequency ω_q indicated.

conduction-electron density, and $E_{\mathrm{F}}=\hbar^2(3\pi^2 n_{3\mathrm{D}}^{\mathrm{e}})^{2/3}/2m_{\mathrm{e}}^*$ is the Fermi energy of electrons at zero temperature. The Hartree energy ($\sim 2E_{\mathrm{F}}/3$) can also be neglected since $E_{\mathrm{F}} \ll E_{\mathrm{G}}$. The higher-order renormalization of $C_{\mathbf{q}}$ by the interaction between electrons and the laser field (phonon-assisted free-carrier absorption) (Ref. 11) is neglected due to the weak electron-phonon interaction at moderate lattice temperature and not too high laser-field intensity. Using Fermi's golden rule[18] for the calculation of the transition rate from the initial state $|i\rangle$ to the final state $|f\rangle$, we obtain

$$\mathcal{W}_{\mathrm{i}\to\mathrm{f}}=\frac{2\pi}{\hbar}|\langle f|\hat{\mathcal{H}}_{\mathrm{I}}(t)|i\rangle|^2\delta(E_{\mathrm{f}}-E_{\mathrm{i}}), \tag{4}$$

where the total energy is conserved for the electron transition process. Hereafter, we will neglect the laser field until it is explicitly indicated.

As shown in Fig. 1, the scattering-in rate for the final electron state $|\mathbf{k}\rangle$ with phonon absorption [see Fig. 1(a)] is calculated as

$$\mathcal{W}^{\mathrm{ab}}_{\mathbf{k}-\mathbf{q}\to\mathbf{k}}=\frac{2\pi}{\hbar}|C_q|^2\delta(E_k^{\mathrm{e}}-\hbar\omega_q-E^{\mathrm{e}}_{|\mathbf{k}-\mathbf{q}|}) \times N_q^{\mathrm{ph}} n^{\mathrm{e}}_{|\mathbf{k}-\mathbf{q}|}(1-n_k^{\mathrm{e}}). \tag{5}$$

On the other hand, the scattering-in rate for the final electron state $|\mathbf{k}\rangle$ with phonon emission [see Fig. 1(b)] is found to be

$$\mathcal{W}^{\mathrm{em}}_{\mathbf{k}+\mathbf{q}\to\mathbf{k}}=\frac{2\pi}{\hbar}|C_q|^2\delta(E_k^{\mathrm{e}}+\hbar\omega_q-E^{\mathrm{e}}_{|\mathbf{k}+\mathbf{q}|}) \times (N_q^{\mathrm{ph}}+1) n^{\mathrm{e}}_{|\mathbf{k}+\mathbf{q}|}(1-n_k^{\mathrm{e}}). \tag{6}$$

Similarly, the scattering-out rate for the initial electron state $|\mathbf{k}\rangle$ with phonon absorption [see Fig. 1(c)] is obtained from

$$\mathcal{W}^{\mathrm{ab}}_{\mathbf{k}\to\mathbf{k}+\mathbf{q}}=\frac{2\pi}{\hbar}|C_q|^2\delta(E^{\mathrm{e}}_{|\mathbf{k}+\mathbf{q}|}-\hbar\omega_q-E_k^{\mathrm{e}}) \times N_q^{\mathrm{ph}}(1-n^{\mathrm{e}}_{|\mathbf{k}+\mathbf{q}|}) n_k^{\mathrm{e}}, \tag{7}$$

and the scattering-out rate for the initial electron state $|\mathbf{k}\rangle$ with phonon emission [see Fig. 1(d)] takes the form of

$$\mathcal{W}^{\mathrm{em}}_{\mathbf{k}\to\mathbf{k}-\mathbf{q}}=\frac{2\pi}{\hbar}|C_q|^2\delta(E^{\mathrm{e}}_{|\mathbf{k}-\mathbf{q}|}+\hbar\omega_q-E_k^{\mathrm{e}}) \times (N_q^{\mathrm{ph}}+1)(1-n^{\mathrm{e}}_{|\mathbf{k}-\mathbf{q}|}) n_k^{\mathrm{e}}. \tag{8}$$

Here, the effect of Pauli exclusion on the final state is taken into account for the electron transition process.

III. DYNAMICS OF PHONON-SCATTERED CONDUCTION ELECTRONS

In this section, we consider the case of no incident laser field. The electron-phonon interaction is included within Fermi's golden rule ($\propto|C_q|^2$). Based on the calculated partial scattering-in and scattering-out rates in Eqs. (5)–(8), we can calculate the total scattering-in rate for the final electron state $|\mathbf{k}\rangle$,

$$\begin{aligned}\mathcal{W}_k^{(\mathrm{in})}&=\sum_{\mathbf{q}}\ (\mathcal{W}^{\mathrm{ab}}_{\mathbf{k}-\mathbf{q}\to\mathbf{k}}+\mathcal{W}^{\mathrm{em}}_{\mathbf{k}+\mathbf{q}\to\mathbf{k}})\\ &=\frac{2\pi}{\hbar}(1-n_k^{\mathrm{e}})\sum_{\mathbf{q}}\ |C_q|^2[\,\delta(E_k^{\mathrm{e}}-\hbar\omega_q-E^{\mathrm{e}}_{|\mathbf{k}-\mathbf{q}|})\\ &\quad\times N_q^{\mathrm{ph}} n^{\mathrm{e}}_{|\mathbf{k}-\mathbf{q}|}+\delta(E_k^{\mathrm{e}}+\hbar\omega_q-E^{\mathrm{e}}_{|\mathbf{k}+\mathbf{q}|})(N_q^{\mathrm{ph}}+1) n^{\mathrm{e}}_{|\mathbf{k}+\mathbf{q}|}],\end{aligned} \tag{9}$$

as well as the total scattering-out rate for the initial electron state $|\mathbf{k}\rangle$,

$$\begin{aligned}\mathcal{W}_k^{(\mathrm{out})}&=\sum_{\mathbf{q}}\ (\mathcal{W}^{\mathrm{em}}_{\mathbf{k}\to\mathbf{k}-\mathbf{q}}+\mathcal{W}^{\mathrm{ab}}_{\mathbf{k}\to\mathbf{k}+\mathbf{q}})\\ &=\frac{2\pi}{\hbar}n_k^{\mathrm{e}}\sum_{\mathbf{q}}\ |C_q|^2[\,\delta(E_k^{\mathrm{e}}+\hbar\omega_q-E^{\mathrm{e}}_{|\mathbf{k}+\mathbf{q}|})\\ &\quad\times N_q^{\mathrm{ph}}(1-n^{\mathrm{e}}_{|\mathbf{k}+\mathbf{q}|})+\delta(E_k^{\mathrm{e}}-\hbar\omega_q-E^{\mathrm{e}}_{|\mathbf{k}-\mathbf{q}|})(N_q^{\mathrm{ph}}+1)\\ &\quad\times(1-n^{\mathrm{e}}_{|\mathbf{k}-\mathbf{q}|})],\end{aligned} \tag{10}$$

where the phonon distribution function is assumed to be in equilibrium and given by

$$N_q^{\mathrm{ph}}=\left[\exp\left(\frac{\hbar\omega_q}{k_{\mathrm{B}}T}\right)-1\right]^{-1}, \tag{11}$$

with lattice temperature T. Using Eqs. (9) and (10), we get the following dynamic equation for the conduction-electron distribution function in the absence of a laser field:

$$\frac{\partial}{\partial t}n_k^{\mathrm{e}}=\mathcal{W}_k^{(\mathrm{in})}-\mathcal{W}_k^{(\mathrm{out})}$$

$$=\frac{2\pi}{\hbar}\sum_{\mathbf{q}}|C_q|^2\delta(E_k^{\mathrm{e}}+\hbar\omega_q-E_{|\mathbf{k}+\mathbf{q}|}^{\mathrm{e}})$$

$$\times[(N_q^{\mathrm{ph}}+1)n_{|\mathbf{k}+\mathbf{q}|}^{\mathrm{e}}(1-n_k^{\mathrm{e}})-N_q^{\mathrm{ph}}n_k^{\mathrm{e}}(1-n_{|\mathbf{k}+\mathbf{q}|}^{\mathrm{e}})]$$

$$+\frac{2\pi}{\hbar}\sum_{\mathbf{q}}|C_q|^2\delta(E_k^{\mathrm{e}}-\hbar\omega_q-E_{|\mathbf{k}-\mathbf{q}|}^{\mathrm{e}})$$

$$\times[N_q^{\mathrm{ph}}n_{|\mathbf{k}-\mathbf{q}|}^{\mathrm{e}}(1-n_k^{\mathrm{e}})-(N_q^{\mathrm{ph}}+1)n_k^{\mathrm{e}}(1-n_{|\mathbf{k}-\mathbf{q}|}^{\mathrm{e}})]. \tag{12}$$

Moreover, we denote that $n_k^{\mathrm{e}}\equiv n^{\mathrm{e}}(E_k^{\mathrm{e}},t)$ and define $f_k^{\mathrm{e}}=\rho_k^{\mathrm{e}}n_k^{\mathrm{e}}$ with the density of states $\rho_k^{\mathrm{e}}=C_0\sqrt{E_k^{\mathrm{e}}}$ in a parabolic-dispersion model, where $C_0=(2m_{\mathrm{e}}^*)^{3/2}/2\pi^2\hbar^3$. If we limit ourselves to the diffusive limit in which $\hbar\omega_q\ll E_k^{\mathrm{e}}$, we obtain the following kinetic Fokker-Planck-type equation for the electron thermal motion in energy space by including only the electron scattering with phonons,

$$\frac{\partial}{\partial t}f_k^{\mathrm{e}}+V_k\frac{\partial}{\partial E_k^{\mathrm{e}}}f_k^{\mathrm{e}}-D_k\frac{\partial^2}{\partial(E_k^{\mathrm{e}})^2}f_k^{\mathrm{e}}=A_kf_k^{\mathrm{e}}+S_k, \tag{13}$$

where the following expansion approximation has been employed:

$$f_{|\mathbf{k}\pm\mathbf{q}|}^{\mathrm{e}}\approx f_k^{\mathrm{e}}\pm\hbar\omega_q\frac{\partial}{\partial E_k^{\mathrm{e}}}f_k^{\mathrm{e}}+\frac{1}{2}(\hbar\omega_q)^2\frac{\partial^2}{\partial(E_k^{\mathrm{e}})^2}f_k^{\mathrm{e}}. \tag{14}$$

In Eq. (13), S_k represents all the other source contributions which will be given in Secs. V and VI, and the dynamical coefficients A_k, V_k, and D_k are defined by

$$A_k=\frac{2\pi}{\hbar}\sum_{\mathbf{q}}|C_q|^2\left\{\delta(E_k^{\mathrm{e}}+\hbar\omega_q-E_{|\mathbf{k}+\mathbf{q}|}^{\mathrm{e}})\left[(N_q^{\mathrm{ph}}+1-n_k^{\mathrm{e}})\left(1-\frac{\hbar\omega_q}{2E_k^{\mathrm{e}}}\right)-N_q^{\mathrm{ph}}\right]\right.$$

$$\left.+\delta(E_k^{\mathrm{e}}-\hbar\omega_q-E_{|\mathbf{k}-\mathbf{q}|}^{\mathrm{e}})\left[(N_q^{\mathrm{ph}}+n_k^{\mathrm{e}})\left(1+\frac{\hbar\omega_q}{2E_k^{\mathrm{e}}}\right)-(N_q^{\mathrm{ph}}+1)\right]\right\}, \tag{15}$$

$$V_k=\frac{2\pi}{\hbar}\sum_{\mathbf{q}}|C_q|^2\hbar\omega_q\left\{\delta(E_k^{\mathrm{e}}-\hbar\omega_q-E_{|\mathbf{k}-\mathbf{q}|}^{\mathrm{e}})(N_q^{\mathrm{ph}}+n_k^{\mathrm{e}})\left(1+\frac{\hbar\omega_q}{2E_k^{\mathrm{e}}}\right)-\delta(E_k^{\mathrm{e}}+\hbar\omega_q-E_{|\mathbf{k}+\mathbf{q}|}^{\mathrm{e}})(N_q^{\mathrm{ph}}+1-n_k^{\mathrm{e}})\left(1-\frac{\hbar\omega_q}{2E_k^{\mathrm{e}}}\right)\right\}, \tag{16}$$

$$D_k=\frac{2\pi}{\hbar}\sum_{\mathbf{q}}|C_q|^2\frac{1}{2}(\hbar\omega_q)^2\left\{\delta(E_k^{\mathrm{e}}+\hbar\omega_q-E_{|\mathbf{k}+\mathbf{q}|}^{\mathrm{e}})(N_q^{\mathrm{ph}}+1-n_k^{\mathrm{e}})\left(1-\frac{\hbar\omega_q}{2E_k^{\mathrm{e}}}\right)+\delta(E_k^{\mathrm{e}}-\hbar\omega_q-E_{|\mathbf{k}-\mathbf{q}|}^{\mathrm{e}})(N_q^{\mathrm{ph}}+n_k^{\mathrm{e}})\left(1+\frac{\hbar\omega_q}{2E_k^{\mathrm{e}}}\right)\right\}. \tag{17}$$

Here, V_k and D_k represent the velocity in energy space of conduction electrons due to power loss in spontaneous-phonon emission and the thermal-diffusion coefficient of electrons in energy space, respectively. As can be seen from Eq. (12), the effect of Pauli exclusion is included in the factors of $1-n_k^{\mathrm{e}}$ and $1-n_{|\mathbf{k}\pm\mathbf{q}|}^{\mathrm{e}}$ for the final electron states during the transitions. If the effect of Pauli exclusion is neglected in Eqs. (13)–(17), we get the same equation as the previously derived quantum kinetic equation[11] by Epifanov *et al.* for the electron-phonon scattering.

The lattice temperature is assumed to be not too high, so that only the scattering with longitudinal phonons is considered by neglecting the umklapp process. For longitudinal optical (LO) phonons in polar semiconductors, we have

$$|C_q|^2=\left(\frac{\hbar\omega_{\mathrm{LO}}}{2\mathcal{V}}\right)\left[\frac{1}{\epsilon_{\mathrm{r}}(\infty)}-\frac{1}{\epsilon_{\mathrm{r}}(0)}\right]\left[\frac{e^2}{\epsilon_0(q^2+Q_{\mathrm{s}}^2)}\right],$$

which reduces to the results for deformation-potential optical (DO) phonon scattering when $q\to 0$,[19] where $1/Q_{\mathrm{s}}$ is the Thomas-Fermi screening length,[17] ω_{LO} is the frequency of the longitudinal optical phonons, and $\epsilon_{\mathrm{r}}(\infty)$ and $\epsilon_{\mathrm{r}}(0)$ are the relative optical and static dielectric constants. On the other hand, for longitudinal acoustic (LA) phonons in both polar and nonpolar semiconductors we have

$$|C_q|^2=\left(\frac{n_{\mathrm{i}}q}{2M_{\mathrm{i}}v_{\mathrm{L}}\mathcal{V}}\right)\left[\frac{e^2}{\epsilon_0\epsilon_{\mathrm{r}}(0)(q^2+Q_{\mathrm{s}}^2)}\right]^2,$$

which approaches the results for deformation-potential acoustic (DA) phonon scattering as $q\to 0$,[19] where M_{i} is the ion mass, n_{i} is the ion density, and v_{s} is the sound velocity of longitudinal acoustic phonons. The weak piezoelectric effect in some semiconductors (e.g., GaAs) with weak inversion-center effect is neglected hereafter at high lattice temperatures.

IV. CORRECTION TO SPONTANEOUS-PHONON EMISSION

In the absence of a laser field, the kinetic Fokker-Planck-type equation (13) for $f_k^{\mathrm{e}}\equiv f^{\mathrm{e}}(E_k^{\mathrm{e}},t)$ only describes the dy-

namics of electrons due to interactions with phonons, where E_k^e is time independent. In this section, we include the effect of the laser field treated classically and find that the intraband transitions of conduction electrons cannot optically respond to the laser field without assistance from phonons. However, we understand that $\langle \mathcal{E}_L(t)\rangle = 0$, but $\langle \mathcal{E}_L^2(t)\rangle \neq 0$ only when $\Omega_L \tau_p \gg 1$, where $\langle \mathcal{A}(t)\rangle$ is the time average of a quantity $\mathcal{A}(t)$ within an interval of collision time τ_p [many time periods of the oscillating field $\mathcal{E}_L(t)$] over which two successive collisions of an electron with phonons can happen. The fact that $\langle \mathcal{E}_L(t)\rangle = 0$ implies no net momentum change of electrons over τ_p after $\mathcal{E}_L(t)$ is applied, which is quite different from the case of a dc electric field. However, $\langle \mathcal{E}_L^2(t)\rangle \neq 0$ indicates a local fluctuation in the electron kinetic energies. We know that the Fokker-Planck-type equation (13) deals with the conduction-electron dynamics (after an ensemble average) over a time scale much longer than τ_p. Since the time period of the laser field $2\pi/\Omega_L$ is much shorter than τ_p, we need to take a time average of the Fokker-Planck-type equation here over many time periods of the laser field. In the presence of a laser field given by $\mathcal{E}_L(t) = \mathcal{E}_{0L}\cos(\Omega_L t)$, where $\mathcal{E}_{0L}$ is the amplitude of the laser field, there exists a local fluctuation in the electron kinetic energies, described by

$$\frac{\partial f_k^e}{\partial t}\Big|_{dr} = \lim_{\Delta t \to 0}\left(\frac{1}{\Delta t}\right)[f^e(E_k^e - (dE_k^e/dt)\Delta t, t) - f^e(E_k^e, t)]$$

$$= -\left\langle \frac{dE_k^e}{dt}\right\rangle \frac{\partial}{\partial E_k^e} f_k^e .$$

Consequently, after an average over many time periods of $\mathcal{E}_L(t)$, the previous Fokker-Planck type equation (13) can be generalized to include this additional energy-drift term $\partial f_k^e/\partial t|_{dr}$ on the right-hand side of the equation, thus yielding

$$\frac{\partial}{\partial t}\overline{f_k^e} + \overline{V}_k \frac{\partial}{\partial E_k^e}\overline{f_k^e} - \overline{D}_k \frac{\partial^2}{\partial (E_k^e)^2}\overline{f_k^e}$$

$$= -\left\langle \frac{dE_k^e}{dt}\right\rangle \frac{\partial}{\partial E_k^e}\overline{f_k^e} + \overline{A}_k \overline{f_k^e} + \overline{S}_k , \qquad (18)$$

where only the slow electron motion compared to τ_p is kept, and $\langle dE_k^e/dt\rangle \propto \langle \mathcal{E}_L^2(t)\rangle$ results from the energy drift of electrons. In Eq. (18), we denote $\overline{f_k^e} \equiv f^e(\overline{E_k^e}, t)$ with nearly time-independent average energy $\overline{E_k^e} = E_k^e - \Delta E_k^e$. We have also assumed that $|\Delta E_k^e| \ll E_k^e$ for the weak local fluctuation in Eq. (18). In principle, Eq. (18) can be applied to study the conduction-electron dynamics between any two successive collisions with phonons provided an expression of ΔE_k^e is given for each scattering event. Instead, we introduce an averaged fluctuation $E_{tr} \equiv \ll \Delta E_k^e \gg$ for the transport of electrons in energy space, which represents the average energy gained from power dissipation of the laser field within semiconductors, where $\langle\langle \mathcal{A}(E_k^e, t)\rangle\rangle \equiv \langle \int dE_k^e \mathcal{A}(E_k^e, t) f_k^e\rangle$ is the average over an ensemble of collisions or over a time scale much longer than τ_p. In this way, E_{tr} becomes a constant on a time scale comparable to τ_p. Using the following expansion under the condition $E_{tr} \ll E_k^e$,

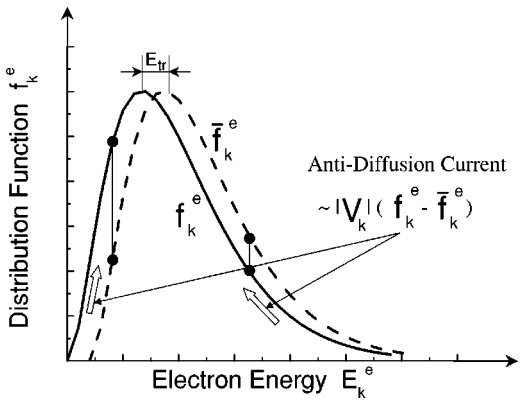

FIG. 2. Illustration of an antidiffusion process, where the solid and dashed curves represent the electron distribution functions f_k^e and $\overline{f_k^e}$, respectively. The dashed curve is a replica of the solid one with a downshift in energy of E_{tr} due to the energy drift in the presence of a laser field. The normal diffusion current always flows down from the maximum of the solid curve. However, the antidiffusion current (two upward hollow arrows), which results from the change of the spontaneous-phonon emission due to energy drift and is proportional to $|\overline{V}_k|(f_k^e - \overline{f_k^e})$, flows up towards the maximum of the solid curve.

$$\overline{f_k^e} \approx f_k^e - E_{tr}\frac{\partial}{\partial E_k^e} f_k^e , \qquad (19)$$

we finally arrive at the generalized Fokker-Planck-type equation in the presence of a laser field after an ensemble average over a time scale much longer than τ_p has been taken:

$$\frac{\partial}{\partial t} f_k^e + V_k^* \frac{\partial}{\partial E_k^e} f_k^e - D_k^* \frac{\partial^2}{\partial (E_k^e)^2} f_k^e = \overline{A}_k f_k^e + \overline{S}_k , \qquad (20)$$

where $\partial \overline{f_k^e}/\partial t \approx \partial f_k^e/\partial t$ since $dE_{tr}/dt \approx 0$. In Eq. (20), the renormalized velocity V_k^* and diffusion coefficient D_k^* in energy space are given by

$$V_k^* = \left\langle \left\langle \frac{dE_k^e}{dt}\right\rangle \right\rangle + \overline{V}_k + E_{tr}\overline{A}_k , \qquad (21)$$

$$D_k^* = \overline{D}_k + E_{tr}\left\langle \left\langle \frac{dE_k^e}{dt}\right\rangle \right\rangle + E_{tr}\overline{V}_k . \qquad (22)$$

The antidiffusion term $E_{tr}\overline{V}_k$ in Eq. (22) results from the correction to the spontaneous-phonon emission from nondrifting (f_k^e) to drifting ($\overline{f_k^e}$) electrons and is proportional to $|\overline{V}_k|(f_k^e - \overline{f_k^e})$. Here $E_{tr}V_k$ plays the role of an antidiffusion process; i.e., the spontaneous-phonon emission decreases when $\partial f_k^e/\partial E_k^e > 0$ but increases as $\partial f_k^e/\partial E_k^e < 0$, as shown in Fig. 2. The antidiffusion term is negative and its magnitude is usually smaller than the field-dependent diffusion coefficient $E_{tr}\langle\langle dE_k^e/dt\rangle\rangle$. Here, the coefficients $\overline{A}_k$, $\overline{V}_k$, and $\overline{D}_k$ are redefined by

$$\overline{A_k}=\frac{2\pi}{\hbar}\sum_{\mathbf{q}}|C_q|^2\Big\{\delta(E_k^{\mathrm{e}}+\hbar\omega_q-E_{|\mathbf{k}+\mathbf{q}|}^{\mathrm{e}})\times\Big[(N_q^{\mathrm{ph}}+1-\overline{n_k^{\mathrm{e}}})\Big(1-\frac{\hbar\omega_q}{2(E_k^{\mathrm{e}}-E_{\mathrm{tr}})}\Big)-N_q^{\mathrm{ph}}\Big]+\delta(E_k^{\mathrm{e}}-\hbar\omega_q-E_{|\mathbf{k}-\mathbf{q}|}^{\mathrm{e}})\times\Big[(N_q^{\mathrm{ph}}+\overline{n_k^{\mathrm{e}}})\Big(1+\frac{\hbar\omega_q}{2(E_k^{\mathrm{e}}-E_{\mathrm{tr}})}\Big)-(N_q^{\mathrm{ph}}+1)\Big]\Big\},\quad(23)$$

$$\overline{V_k}=\frac{2\pi}{\hbar}\sum_{\mathbf{q}}|C_q|^2\hbar\omega_q\Big\{\delta(E_k^{\mathrm{e}}-\hbar\omega_q-E_{|\mathbf{k}-\mathbf{q}|}^{\mathrm{e}})(N_q^{\mathrm{ph}}+\overline{n_k^{\mathrm{e}}})\times\Big(1+\frac{\hbar\omega_q}{2(E_k^{\mathrm{e}}-E_{\mathrm{tr}})}\Big)-\delta(E_k^{\mathrm{e}}+\hbar\omega_q-E_{|\mathbf{k}+\mathbf{q}|}^{\mathrm{e}})\times(N_q^{\mathrm{ph}}+1-\overline{n_k^{\mathrm{e}}})\Big(1-\frac{\hbar\omega_q}{2(E_k^{\mathrm{e}}-E_{\mathrm{tr}})}\Big)\Big\},\quad(24)$$

$$\overline{D_k}=\frac{2\pi}{\hbar}\sum_{\mathbf{q}}|C_q|^2\frac{1}{2}(\hbar\omega_q)^2\times\Big\{\delta(E_k^{\mathrm{e}}+\hbar\omega_q-E_{|\mathbf{k}+\mathbf{q}|}^{\mathrm{e}})(N_q^{\mathrm{ph}}+1-\overline{n_k^{\mathrm{e}}})\times\Big(1-\frac{\hbar\omega_q}{2(E_k^{\mathrm{e}}-E_{\mathrm{tr}})}\Big)+\delta(E_k^{\mathrm{e}}-\hbar\omega_q-E_{|\mathbf{k}-\mathbf{q}|}^{\mathrm{e}})\times(N_q^{\mathrm{ph}}+\overline{n_k^{\mathrm{e}}})\Big(1+\frac{\hbar\omega_q}{2(E_k^{\mathrm{e}}-E_{\mathrm{tr}})}\Big)\Big\},\quad(25)$$

where $\overline{n_k^{\mathrm{e}}}\equiv n^{\mathrm{e}}(E_k^{\mathrm{e}}-E_{\mathrm{tr}},t)$. In addition, we find

$$\Big\langle\Big\langle\frac{d}{dt}E_k^{\mathrm{e}}\Big\rangle\Big\rangle=\Big\langle\Big\langle\mathbf{v}_k^{\mathrm{e}}\cdot m_{\mathrm{e}}^*\frac{d}{dt}\mathbf{v}_k^{\mathrm{e}}\Big\rangle\Big\rangle=\frac{1}{3}\sigma_{\mathrm{c}}(\Omega_{\mathrm{L}})\mathcal{E}_{\mathrm{L}}^2,\quad(26)$$

from which we obtain $E_{\mathrm{tr}}\approx\sigma_{\mathrm{c}}(\Omega_{\mathrm{L}})\mathcal{E}_{\mathrm{L}}^2\tau_{\mathrm{p}}/3$ (τ_{p} is here regarded as an ensemble-average relaxation time). Further, we find

$$E_{\mathrm{tr}}\Big\langle\Big\langle\frac{d}{dt}E_k^{\mathrm{e}}\Big\rangle\Big\rangle\approx\Big\langle\Big\langle\Delta E_k^{\mathrm{e}}\frac{d}{dt}E_k^{\mathrm{e}}\Big\rangle\Big\rangle=\Big\langle\Big\langle\Delta E_k^{\mathrm{e}}\mathbf{v}_k^{\mathrm{e}}\cdot m_{\mathrm{e}}^*\frac{d}{dt}\mathbf{v}_k^{\mathrm{e}}\Big\rangle\Big\rangle\approx\frac{2}{3}\sigma_{\mathrm{c}}(\Omega_{\mathrm{L}})\mathcal{E}_{\mathrm{L}}^2E_k^{\mathrm{e}}.\quad(27)$$

In Eqs. (26) and (27), we have used the fact that $\langle\langle\mathbf{v}_k^{\mathrm{e}}\cdot m_{\mathrm{e}}^*d\mathbf{v}_k^{\mathrm{e}}/dt\rangle\rangle=(e/3)\langle\langle v_k^{\mathrm{e}}\mathcal{E}_{\mathrm{L}}(t)\rangle\rangle=\sigma_{\mathrm{c}}(\Omega_{\mathrm{L}})\mathcal{E}_{\mathrm{L}}^2/3$ from the Drude model $e\langle\langle v_k^{\mathrm{e}}\mathcal{E}_{\mathrm{L}}(t)\rangle\rangle=\langle\mathcal{E}_{\mathrm{L}}^2(t)\rangle\sigma_{\mathrm{c}}(\Omega_{\mathrm{L}})$, where $\mathcal{E}_{\mathrm{L}}^2=\mathcal{E}_{0\mathrm{L}}^2/2$, and the ac Drude conductivity in Eqs. (26) and (27) is given by

$$\sigma_{\mathrm{c}}(\Omega_{\mathrm{L}})=\frac{e^2\tau_{\mathrm{p}}}{m_{\mathrm{e}}^*(1+\Omega_{\mathrm{L}}^2\tau_{\mathrm{p}}^2)}.\quad(28)$$

Here $\sigma_{\mathrm{c}}(\Omega_{\mathrm{L}})$ tends to $e^2/m_{\mathrm{e}}^*\Omega_{\mathrm{L}}^2\tau_p$ when $\Omega_{\mathrm{L}}\tau_p\gg1$.

The energy-drift phenomenon for conduction electrons is a classical joule heating effect due to power dissipation of the laser field within semiconductors, which justifies the use of the Drude model for the energy-drift effect in Eq. (26). It is completely different from the absorption of photons by either interband or intraband electron transitions. We also know that there is no intraband free-carrier absorption of photons without assistance from phonons. The effect of phonon-assisted intraband free-carrier absorption of photons renormalizes the electron-phonon interaction and is calculated as $\sim|C_q|^2N_q^{\mathrm{ph}}[e^2\mathcal{E}_{0\mathrm{L}}^2q^2/(m_{\mathrm{e}}^*\Omega_{\mathrm{L}}^2)^2]\exp(-\sqrt{2m_{\mathrm{e}}^*v_{\mathrm{s}}^2E_{\mathrm{G}}}/k_{\mathrm{B}}T)$ to leading order. Therefore, if the condition $e\mathcal{E}_{0\mathrm{L}}\ll(\hbar v_sm_{\mathrm{e}}^*\Omega_{\mathrm{L}}^2/k_{\mathrm{B}}T)\exp(\sqrt{m_{\mathrm{e}}^*v_{\mathrm{s}}^2E_{\mathrm{G}}}/2k_{\mathrm{B}}T)$ is satisfied, this effect becomes negligible compared to the contributions from electron-phonon scattering described in Sec. III.

By including the effect of energy drift of conduction electrons in Eq. (18), both joule heating $\langle\langle dE_k^{\mathrm{e}}/dt\rangle\rangle$ and the field-dependent diffusion $E_{\mathrm{tr}}\ll dE_k^{\mathrm{e}}/dt\rangle\rangle$ of electrons are systematically derived in Eqs. (21) and (22) instead of including them in the equation phenomenologically. More importantly, the new contribution $E_{\mathrm{tr}}\overline{V_k}$ from the antidiffusion process as a correction to the spontaneous-phonon emission arises in Eq. (22). The amplitude $\mathcal{E}_{0\mathrm{L}}$ of the pulsed laser field introduced in this paper should be time dependent. We assume a standard Gaussian profile (with unit peak strength) for the intensity ($\propto\mathcal{E}_{0\mathrm{L}}^2$) of the pulsed laser field. Therefore, the time dependence of the laser intensity is characterized by both the peak intensity I_{L} and the pulse duration τ_{L} We label the time by the deviation from the moment of peak intensity.

V. STIMULATED INTERBAND ABSORPTION OF PHOTONS

The previous theories[1,11,13] are most often applied to a dielectric with a huge E_{G}, thereby allowing only multiphoton excitations to be considered. For semiconductors, however, E_{G} can be moderate (GaAs) or even narrow (GaSb). In these cases, single-photon excitation becomes possible. In contrast to intraband transitions, interband electron transitions between the conduction and valence bands can respond to the laser field directly if the laser photon energy $\hbar\Omega_{\mathrm{L}}$ is larger than E_{G}. This contributes to the source term $\overline{S_k}$ in Eq. (20), which usually depends only on electron-energy change. Hereafter, we will simply write it as S_k and denote the direct coherent interband excitation by $S_k^{(1)}$. Fermi's golden rule ($\propto|F_k|^2$) leads us to

$$S_k^{(1)}=\frac{2\pi}{\hbar}|F_k|^2\mathcal{P}_k^{\mathrm{e}}\Big[\frac{2|F_k|/\pi}{(\hbar\Omega_{\mathrm{L}}-E_k^{\mathrm{e}}-E_k^{\mathrm{h}}-E_{\mathrm{G}})^2+4|F_k|^2}\Big],\quad(29)$$

where $\mathcal{P}_k^{\mathrm{e}}=\rho_k^{\mathrm{e}}-2f_k^{\mathrm{e}}$ if $\rho_k^{\mathrm{e}}\geqslant2f_k^{\mathrm{e}}$ for Pauli exclusion or zero if $\rho_k^{\mathrm{e}}<2f_k^{\mathrm{e}}$ for saturated absorption, $4|F_k|^2$ in the denominator of Eq. (29) is the power broadening due to the laser field in the interband transition of electrons,[16] E_k^{h} is the hole energy in the valence band, and[20]

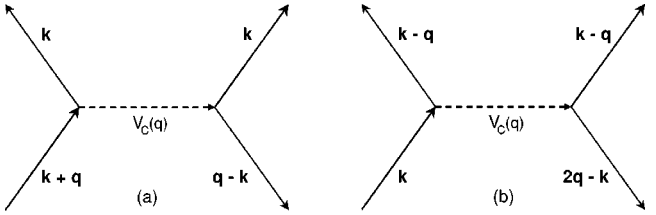

FIG. 3. Diagrams for impact ionization with electron scattering into state $|\mathbf{k}\rangle$ in (a) and scattering out of state $|\mathbf{k}\rangle$ in (b). Here, the upward and downward solid arrows represent the electron and hole states with the wave vector indicated, respectively. The horizontal dashed arrows stand for the Coulomb interaction $V_{\mathrm{C}}(q)$ between two electrons.

$$|F_k|^2 \approx \frac{e^2\mathcal{E}_{\mathrm{L}}^2}{m_0\Omega_{\mathrm{L}}^2}\left[\left(\frac{m_0}{m_{\mathrm{e}}^*}-1\right)\frac{E_{\mathrm{G}}(E_{\mathrm{G}}+\Delta_0)}{2(E_{\mathrm{G}}+2\Delta_0/3)}\right] \tag{30}$$

with free-electron mass m_0 and the spin-orbit splitting Δ_0 of the bulk semiconductor. The hole energy is much smaller than the electron energy due to its very heavy effective mass and can be set to zero as an approximation.

VI. COULOMB SCATTERING AND DAMAGE

In Secs. III and V, we included Fermi's golden rule for interactions between electrons and phonons ($\propto|C_q|^2$) and between electrons and a laser field ($\propto|F_k|^2$), respectively. In this section, we will include source terms to the Fokker-Planck-type equation (20) derived using second-order perturbation theory, such as Coulomb scattering [$\propto|V_{\mathrm{C}}(q)|^2$], which is very important to conduction-electron dynamics and the change of electron density. The next-higher-order electron scattering through phonon-mediated interactions ($\propto|C_q|^4$) is very small and can be neglected due to weak interactions between electrons and phonons.

A. Impact ionization

Impact ionization is a second-order two-particle Coulomb scattering process proportional to $|V_{\mathrm{C}}(q)|^2$. As shown in Fig. 3, the scattering-in rate for final electron state $|\mathbf{k}\rangle$ [see Fig. 3(a)] is calculated as

$$\begin{aligned}\Gamma_{\mathrm{imp}}^{(\mathrm{in})}(\mathbf{k},\mathbf{q}) &= N_{\mathrm{eff}}^{\mathrm{e}}\frac{2\pi}{\hbar}(1-n_k^{\mathrm{e}})^2|V_{\mathrm{C}}(q)|^2 g_{\mathrm{v}}(q)\\ &\times\delta(2E_k^{\mathrm{e}}-E_{|\mathbf{k}+\mathbf{q}|}^{\mathrm{e}}+E_{\mathrm{G}}+E_{|\mathbf{k}-\mathbf{q}|}^{\mathrm{h}})\\ &\times(1-n_{|\mathbf{k}-\mathbf{q}|}^{\mathrm{h}})n_{|\mathbf{k}+\mathbf{q}|}^{\mathrm{e}},\end{aligned} \tag{31}$$

where $N_{\mathrm{eff}}^{\mathrm{e}}$ is the effective number of conduction electrons with energy close to E_{G}, $V_{\mathrm{C}}(q)=e^2/[\epsilon_0\epsilon_{\mathrm{r}}(0)q^2\mathcal{V}]$ is the Fourier transform of the Coulomb potential, and $g_{\mathrm{v}}(q)$ is the interband-transition form factor. Similarly, the scattering-out rate for initial electron state $|\mathbf{k}\rangle$ [see Fig. 3(b)] is found to be

$$\begin{aligned}\Gamma_{\mathrm{imp}}^{(\mathrm{out})}(\mathbf{k},\mathbf{q}) &= N_{\mathrm{eff}}^{\mathrm{e}}\frac{2\pi}{\hbar}n_k^{\mathrm{e}}|V_{\mathrm{C}}(q)|^2 g_{\mathrm{v}}(q)\,\delta(2E_{|\mathbf{k}-\mathbf{q}|}^{\mathrm{e}}-E_k^{\mathrm{e}}+E_{\mathrm{G}}\\ &+E_{|\mathbf{k}-2\mathbf{q}|}^{\mathrm{h}})(1-n_{|\mathbf{k}-\mathbf{q}|}^{\mathrm{e}})^2(1-n_{|\mathbf{k}-2\mathbf{q}|}^{\mathrm{h}}).\end{aligned} \tag{32}$$

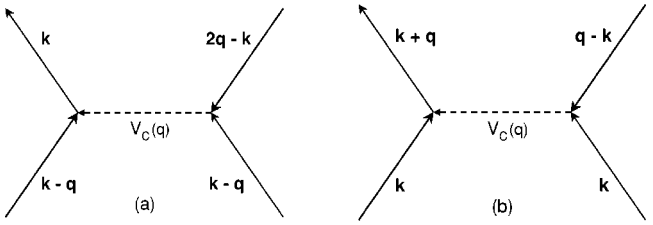

FIG. 4. Diagrams for Auger recombination with electron scattering into state $|\mathbf{k}\rangle$ in (a) and scattering out of state $|\mathbf{k}\rangle$ in (b). Here, the upward and downward solid arrows represent the electron and hole states with the wave vector indicated, respectively. The horizontal dashed arrows stand for the effective phonon-mediated interaction $U_{\mathrm{eff}}(\mathbf{q})$ between two electrons.

Finally, we obtain $\Gamma_k^{(\mathrm{in})}=\Sigma_{\mathbf{q}}\Gamma_{\mathrm{imp}}^{(\mathrm{in})}(\mathbf{k},\ \mathbf{q})$ and $\Gamma_k^{(\mathrm{out})}=\Sigma_{\mathbf{q}}\Gamma_{\mathrm{imp}}^{(\mathrm{out})}(\mathbf{k},\ \mathbf{q})$. As a result, the source contribution $S_k^{(2)}$ from impact ionization is given by

$$\begin{aligned}S_k^{(2)} &= \rho_k^{\mathrm{e}}(\Gamma_k^{(\mathrm{in})}-\Gamma_k^{(\mathrm{out})})\\ &= I_k^{(1)}f^{\mathrm{e}}(2E_k^{\mathrm{e}}+E_{\mathrm{G}},t)-I_k^{(2)}f^{\mathrm{e}}(E_k^{\mathrm{e}},t)\\ &= N_{\mathrm{eff}}^{\mathrm{e}}\frac{2\pi}{\hbar}\sum_{\mathbf{q}}|V_{\mathrm{C}}(q)|^2 g_{\mathrm{v}}(q)\\ &\times\Big[\delta(2E_k^{\mathrm{e}}-E_{|\mathbf{k}+\mathbf{q}|}^{\mathrm{e}}+E_{\mathrm{G}}+E_{|\mathbf{k}-\mathbf{q}|}^{\mathrm{h}})(1-n_k^{\mathrm{e}})^2\\ &\times(1-n_{|\mathbf{k}-\mathbf{q}|}^{\mathrm{h}})\sqrt{\frac{E_k^{\mathrm{e}}}{2E_k^{\mathrm{e}}+E_{\mathrm{G}}+E_{|\mathbf{k}-\mathbf{q}|}^{\mathrm{h}}}}\\ &\times f^{\mathrm{e}}(2E_k^{\mathrm{e}}+E_{\mathrm{G}}+E_{|\mathbf{k}-\mathbf{q}|}^{\mathrm{h}},t)-\delta(2E_{|\mathbf{k}-\mathbf{q}|}^{\mathrm{e}}-E_k^{\mathrm{e}}+E_{\mathrm{G}}+E_k^{\mathrm{h}})\\ &\times(1-n_k^{\mathrm{h}})(1-n_{|\mathbf{k}-\mathbf{q}|}^{\mathrm{e}})^2 f^{\mathrm{e}}(E_k^{\mathrm{e}},t)\Big].\end{aligned} \tag{33}$$

We have defined the coefficients in Eq. (33) as

$$\begin{aligned}I_k^{(1)} &\approx n_{3\mathrm{D}}^{\mathrm{e}}\mathcal{V}\frac{2\pi}{\hbar}\left(\frac{2m_{\mathrm{e}}^*}{m_0}\right)\sqrt{\frac{E_k^{\mathrm{e}}}{2E_k^{\mathrm{e}}+E_{\mathrm{G}}}}\sum_{\mathbf{q}}|V_{\mathrm{C}}(q)|^2\\ &\times\delta(2E_k^{\mathrm{e}}-E_{|\mathbf{k}+\mathbf{q}|}^{\mathrm{e}}+E_{\mathrm{G}}),\\ I_k^{(2)} &\approx n_{3\mathrm{D}}^{\mathrm{e}}\mathcal{V}\frac{2\pi}{\hbar}\left(\frac{2m_{\mathrm{e}}^*}{m_0}\right)\sum_{\mathbf{q}}|V_{\mathrm{C}}(q)|^2\delta(2E_{|\mathbf{k}-\mathbf{q}|}^{\mathrm{e}}-E_k^{\mathrm{e}}+E_{\mathrm{G}}),\end{aligned}$$

where we have assumed that $m_{\mathrm{h}}^*\to\infty$ and $g_{\mathrm{v}}(q)\approx 2(m_{\mathrm{e}}^*/m_0)$.

B. Auger recombination

The electron-electron interaction which leads to Auger recombination was included phenomenologically in our previous work.[21] The recombination rate was derived based on the existing impact ionization model[22] via detailed balance. The Auger recombination process is also a second-order two-particle Coulomb scattering process proportional to $|V_{\mathrm{C}}(q)|^2$. As we can see from Fig. 4, the scattering-in rate

for a final electron state $|\mathbf{k}\rangle$ [see Fig. 4(a)] is

$$\Gamma_{\mathrm{rec}}^{(\mathrm{in})}(\mathbf{k},\mathbf{q})=\frac{2\pi}{\hbar}(1-n_k^{\mathrm{e}})n_{|\mathbf{k}-2\mathbf{q}|}^{\mathrm{h}}|V_{\mathrm{C}}(q)|^2 g_{\mathrm{v}}(q) \times\delta(E_k^{\mathrm{e}}-2E_{|\mathbf{k}-\mathbf{q}|}^{\mathrm{e}}-E_{\mathrm{G}}-E_{|\mathbf{k}-2\mathbf{q}|}^{\mathrm{h}})(n_{|\mathbf{k}-\mathbf{q}|}^{\mathrm{e}})^2. \tag{34}$$

Similarly, the scattering-out rate for an initial electron state $|\mathbf{k}\rangle$ [see Fig. 4(b)] is found to be

$$\Gamma_{\mathrm{rec}}^{(\mathrm{out})}(\mathbf{k},\mathbf{q})=\frac{2\pi}{\hbar}(n_k^{\mathrm{e}})^2|V_{\mathrm{C}}(q)|^2 g_{\mathrm{v}}(q)\,\delta(E_{|\mathbf{k}+\mathbf{q}|}^{\mathrm{e}}-2E_k^{\mathrm{e}}-E_{\mathrm{G}} -E_{|\mathbf{k}-\mathbf{q}|}^{\mathrm{h}})(1-n_{|\mathbf{k}+\mathbf{q}|}^{\mathrm{e}})n_{|\mathbf{k}-\mathbf{q}|}^{\mathrm{h}}. \tag{35}$$

Finally, we arrive at $\Gamma_k^{(\mathrm{in})}=\Sigma_{\mathbf{q}}\Gamma_{\mathrm{rec}}^{(\mathrm{in})}(\mathbf{k},\ \mathbf{q})$ and $\Gamma_k^{(\mathrm{out})}=\Sigma_{\mathbf{q}}\Gamma_{\mathrm{rec}}^{(\mathrm{out})}(\mathbf{k},\ \mathbf{q})$. As a result, the source contribution $S_k^{(3)}$ from Auger recombination is given by

$$\begin{aligned}S_k^{(3)}&=\rho_k^{\mathrm{e}}(\Gamma_k^{(\mathrm{in})}-\Gamma_k^{(\mathrm{out})})\\&=R_k^{(1)}\{f^{\mathrm{e}}[(E_k^{\mathrm{e}}-E_{\mathrm{G}})/2,t]\}^2-R_k^{(2)}\{f^{\mathrm{e}}(E_k^{\mathrm{e}},t)\}^2\\&=\frac{2\pi}{\hbar}\sum_{\mathbf{q}}|V_{\mathrm{c}}(q)|^2 g_{\mathrm{v}}(q)\Bigg\{\delta(E_k^{\mathrm{e}}-2E_{|\mathbf{k}-\mathbf{q}|}^{\mathrm{e}}-E_{\mathrm{G}}-E_{|\mathbf{k}-2\mathbf{q}|}^{\mathrm{h}})(1-n_k^{\mathrm{e}})n_{|\mathbf{k}-2\mathbf{q}|}^{\mathrm{h}}\left[\frac{2E_k^{\mathrm{e}}}{\rho_k^{\mathrm{e}}(E_k^{\mathrm{e}}-E_{\mathrm{G}}-E_{|\mathbf{k}-2\mathbf{q}|}^{\mathrm{h}})}\right]\\&\times\left[f^{\mathrm{e}}\left(\frac{1}{2}(E_k^{\mathrm{e}}-E_{\mathrm{G}}-E_{|\mathbf{k}-2\mathbf{q}|}^{\mathrm{h}}),t\right)\right]^2-\delta(E_{|\mathbf{k}-\mathbf{q}|}^{\mathrm{e}}-2E_k^{\mathrm{e}}-E_{\mathrm{G}}-E_{|\mathbf{k}+\mathbf{q}|}^{\mathrm{h}})(1-n_{|\mathbf{k}-\mathbf{q}|}^{\mathrm{e}})n_{|\mathbf{k}+\mathbf{q}|}^{\mathrm{h}}\left(\frac{1}{\rho_k^{\mathrm{e}}}\right)[f^{\mathrm{e}}(E_k^{\mathrm{e}},t)]^2\Bigg\}.\end{aligned} \tag{36}$$

In Eq. (36) we have defined the following coefficients:

$$R_k^{(1)}\approx n_{3\mathrm{D}}^{\mathrm{e}}\mathcal{V}\frac{2\pi}{\hbar}\left(\frac{2m_{\mathrm{e}}^*}{m_0}\right)\left[\frac{2E_k^{\mathrm{e}}}{\rho_k^{\mathrm{e}}(E_k^{\mathrm{e}}-E_{\mathrm{G}})}\right]\sum_{\mathbf{q}}|V_{\mathrm{c}}(q)|^2 n_{|\mathbf{k}-2\mathbf{q}|}^{\mathrm{h}} \times\delta(E_k^{\mathrm{e}}-2E_{|\mathbf{k}-\mathbf{q}|}^{\mathrm{e}}-E_{\mathrm{G}}),$$

$$R_k^{(2)}\approx n_{3\mathrm{D}}^{\mathrm{e}}\mathcal{V}\frac{2\pi}{\hbar}\left(\frac{2m_{\mathrm{e}}^*}{m_0}\right)\left(\frac{1}{\rho_k^{\mathrm{e}}}\right)\sum_{\mathbf{q}}|V_{\mathrm{c}}(q)|^2 n_{|\mathbf{k}+\mathbf{q}|}^{\mathrm{h}} \times\delta(E_{|\mathbf{k}-\mathbf{q}|}^{\mathrm{e}}-2E_k^{\mathrm{e}}-E_{\mathrm{G}}),$$

where we have assumed that $m_{\mathrm{h}}^*\to\infty$ and $g_{\mathrm{v}}(q)\approx 2(m_{\mathrm{e}}^*/m_0)$. The contribution from Auger recombination in Eq. (36) is very small compared with that from the impact ionization in Eq. (33) due to a negligible population of holes at large momenta. Combining the results in Secs. V and VI, we obtain the total source term $\overline{S_k}\approx S_k^{(1)}+S_k^{(2)}+S_k^{(3)}$ under $\overline{A_k}\approx 0$.

C. Laser damage in semiconductors

In this part, we would like to discuss some possible types of damage in semiconductors. The discussion below includes optical, electrical, and structural damage possibilities.

If an incident light field is absorbed by an intrinsic (undoped) bulk semiconductor, the electrons in the completely filled valence band will transit upward to the conduction band. The free-electron density increases with the intensity of the incident light. The excited electrons in the conduction band can form an electron plasma when the density is high and thus the Coulomb interaction is strong. The existence of this plasma increases the reflection of the incident light. When the condition

$$\Omega_{\mathrm{L}}^2\geqslant\frac{e^2 n_{3\mathrm{D}}^{\mathrm{e}}}{\epsilon_0\epsilon_{\mathrm{r}}(0)m_{\mathrm{e}}^*}$$

is satisfied, the incident light will be totally reflected from the surface of the semiconductor. At this point, the semiconductor becomes opaque, and the electron density reaches its maximum value $n_{\mathrm{c}}^{\mathrm{opt}}$. In this case, we call the opaque semiconductor optically damaged by the laser field for optoelectronic uses since the incident light can no longer be coupled into it. For $\hbar\Omega_{\mathrm{L}}=E_{\mathrm{G}}=1.42$ eV (for GaAs), we get $n_{\mathrm{c}}^{\mathrm{opt}}=1.3\times 10^{23}\ \mathrm{cm}^{-3}$.

An intrinsic (undoped) semiconductor behaves like an insulator at low temperatures, but it becomes a good conductor at room temperature ($T=300$ K). The thermally excited conduction-electron density in intrinsic semiconductors under equilibrium is found to be

$$N_{\mathrm{I}}=\sqrt{N_{\mathrm{C}}N_{\mathrm{V}}}\exp\left(-\frac{E_{\mathrm{G}}}{2k_{\mathrm{B}}T}\right),$$

where $N_{\mathrm{V}}=2(m_{\mathrm{e}}^*k_{\mathrm{B}}T/2\pi\hbar^2)^{3/2}$ and $N_{\mathrm{C}}=2(m_{\mathrm{e}}^*k_{\mathrm{B}}T/2\pi\hbar^2)^{3/2}$ are the state densities of holes and electrons, respectively. N_{I} is found to increase with T. Here N_{I} reaches its maximum value through thermal excitation at T_m (melting temperature) and is denoted by $n_{\mathrm{c}}^{\mathrm{elec}}$. At this point, a huge current under a small bias will be produced in a circuit utilizing this host semiconductor. The conduction electrons can be equivalently produced by a laser field instead of by thermal excitation to give rise to the same electron density $n_{\mathrm{c}}^{\mathrm{elec}}$. In this case, we

call the semiconductor electrically damaged by the laser field for transistor uses. For GaAs, we find $T_m = 1512$ K, and thereby we get $n_c^{elec} = 8.7 \times 10^{17}$ cm^{-3} which is much smaller than n_c^{opt} for $E_G = 1.42$ eV.

The atoms in most semiconductors, such as Si and GaAs, are chemically connected by covalent bonds with cohesive energy $V_B \sim E_G$ in a crystal since E_G prohibits the creation of free electrons from bound electrons in the valence band. If the intrinsic semiconductors are exposed to an incident laser field, the statistically averaged kinetic energy per electron can be written as

$$\langle E_k^e \rangle = \left(\int_0^{+\infty} E_k^e f_k^e dE_k^e \right) \Big/ \left(\int_0^{+\infty} f_k^e dE_k^e \right),$$

which is related to the electron temperature T_e by $\Delta\overline{E} = \langle E_k^e \rangle - 3E_F/5 = 3k_B T_e/2$, where $E_F = \hbar^2 (3\pi^2 n_{3D}^e)^{2/3}/2m_e^*$ is the Fermi energy of conduction electrons at zero temperature. When the electron distribution function f_k^e peaks at higher and higher energies, $\Delta\overline{E}$ increases although n_{3D}^e can be very small at this time. If $\langle E_k^e \rangle = E_G$, there is an instability for chemical bonds in semiconductors. In this case, we call the semiconductor structurally damaged by the laser field for semiconducting-material uses.

VII. NUMERICAL RESULTS AND DISCUSSIONS

In the following numerical calculations, we choose a bulk GaAs semiconductor sample although the theory presented in this paper applies to most semiconductors. The parameters for our calculations are listed as follows: $T = 300$ K, $E_G = 1.42$ eV at $T = 300$ K (1.50 eV at $T = 100$ K), $\Delta_0 = 0.43$ eV, $\tau_p = 0.66$ ps, $I_L = 8 \times 10^{15}$ W/m^2, $\hbar\Omega_L - E_G = 200$ meV, $\tau_L = 1$ ps, $m_e^* = 0.067\ m_0$, $m_h^* = 0.62\ m_0$, $\epsilon_r(0) = 13.18$, $\epsilon_r(\infty) = 10.89$, $\hbar\omega_{LO} = 36.25$ meV, $v_s = 5.14 \times 10^5$ cm/s, $n_i = 2.22 \times 10^{22}$ cm^{-3}, and $M_i = 2.4 \times 10^{-25}$ kg. For a peak intensity $I_L = 8 \times 10^{15}$ W/m^2, we find from calculations that the conduction-electron density n_e^{3D} satisfies $n_c^{elec} < n_e^{3D} < n_c^{opt}$. This implies that the semiconductor suffers from electrical damage but not optical damage. Moreover, we find that the average kinetic energy per electron $\langle E_k^e \rangle$ is always smaller than E_G, which implies that the semiconductor is structurally stable. We denote a dimensionless time t/τ_L by $\tilde{t}$ as the deviation from the moment of peak intensity and a dimensionless kinetic energy E_k^e/E_G by $\tilde{E}$.

The current theory compared with previous theories[2–6,8–13] has introduced an antidiffusion term arising from the correction to the spontaneous-phonon emission from the drifting electrons. Figure 5 displays the effect of the antidiffusion process on the electron distribution function f_k^e as a function of $\tilde{E}$ by including the antidiffusion term $E_{tr}\overline{V}_k$ in the total diffusion coefficient D_k^* in Eq. (22). Compared to $\tilde{t} = -1.25$ in (a) where the laser field is weak, we see in (b) that when $\tilde{t} = -0.5$, a ''kink'' is developed in f_k^e on the low-energy side of the peak as a result of the competition between the upward antidiffusion and the downward thermal diffusion $\overline{D}_k$ (large at low energies and high temperatures) for $E_{tr} \sim k_B T$ (see Fig. 2). When the laser field is further increased in (c) ($\tilde{t} = 0.1$), the field-dependent diffusion starts to take the role of the thermal diffusion for $E_{tr} \gg k_B T$ and $\langle\langle dE_k^e/dt \rangle\rangle / |\overline{V}_k| > 1$. In this case, the strength of the kink is relatively reduced by transferring the electrons above the kink to the peak in both (c) and (d). The laser-induced changes observed in f_k^e in Fig. 5 are also visible in Fig. 6. Here, the electron density n_{3D}^e in (a) as a function of $\tilde{t}$ displays a slight increase for $\tilde{t} > -0.5$ when the antidiffusion process is included (solid curve). This results from the fact that the effect of the impact ionization is actually enhanced by moving electrons up from the edge of the conduction band due to the upward antidiffusion energy current. The average electron kinetic energy $\langle E_k^e \rangle$ in (b) reflects the shape change of f_k^e even though n_{3D}^e (area under the f_k^e curve) is a constant with time. The solid curve in (b) starts peeling off the dashed curve around $\tilde{t} = -1.0$ due to the development of a kinklike feature at low energies. Later, the solid curve merges with the dashed curve for $\tilde{t} > 0$ due to the relatively reduced strength of the kink and the dominant enhancement of the peak. In the following, we will keep the antidiffusion term $E_{tr}\overline{V}_k$ as our standard calculation which includes all the terms. In comparison with the standard calculation, we study different effects by turning off the relevant term in our calculations.

It is known that the Auger recombination that results from the Coulomb interaction between two electrons can reduce the electron density in the conduction band. From our calculation, we find that the recombination reduces the occupation of electrons at the band edge (dominant there) and suppresses a spikelike feature there to a kink. Combined with the thermal and field-dependent diffusion as well as the thermal emission, the recombination greatly decreases the occupation of low-energy electrons and shifts up the peak in f_k^e. The dramatic decrease of n_{3D}^e at the peak intensity is an indication of the efficient recombination. On the other hand, by removing low-energy electrons through recombination, the evident increase of $\langle E_k^e \rangle$ is seen before the peak intensity is reached, which is the combined result of both shifting up the peak and suppressing the spikelike feature.

From Fig. 5, we find that the competition between thermal diffusion and antidiffusion is one of the reasons for the formation of the kinklike feature on the low-energy side of the peak. From our calculation, we find that the thermal diffusion at early times only causes a slight reduction of the peak strength and a shifting-up of the peak position. With increasing peak intensity of the laser field, the downward thermal diffusion induces a kinklike feature around the band edge. Simultaneously, it somewhat reduces the peak strength of f_k^e. The downward thermal diffusion promotes the occupation of electrons near the band edge and greatly speeds up the Auger recombination process. It is found that efficient Auger recombination at the band edge overcomes the increase of electrons from the thermal diffusion. Consequently, the band edge spike is suppressed into a kink.

The main energy-loss mechanism for conduction elec-

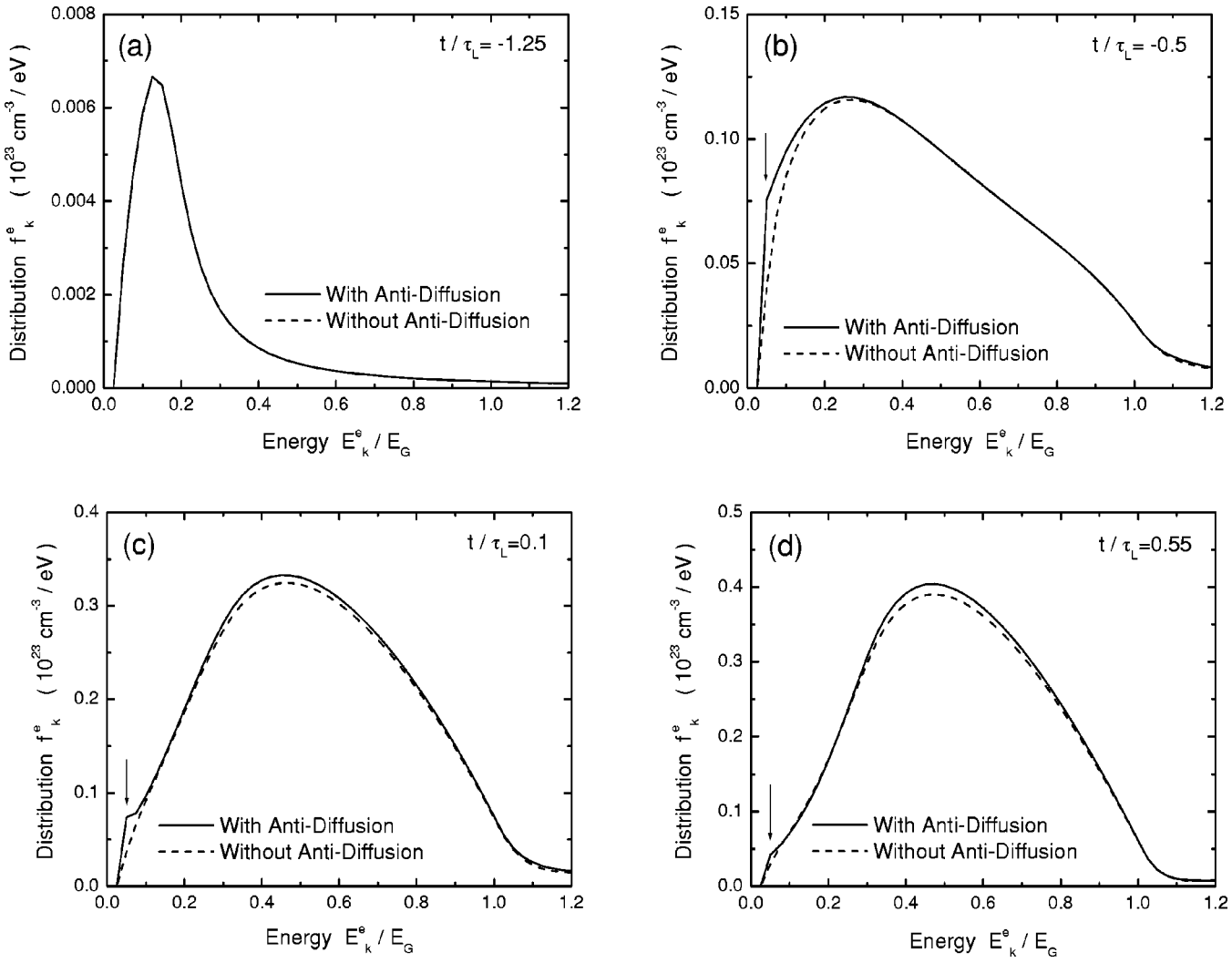

FIG. 5. Comparison of f_k^e as a function of E_k^e/E_G at four different times of a laser pulse by including (solid curves) or excluding (dashed curves) an antidiffusion current. The four times set in (a), (b), (c), and (d) are $t/\tau_L = -1.25$, -0.5, 0.1, and 0.55, respectively. Here, the laser pulse is assumed to peak at $t=0$. The vertical arrows in the figures indicate the kinklike feature described in the text. The parameters for our calculations are given in the text.

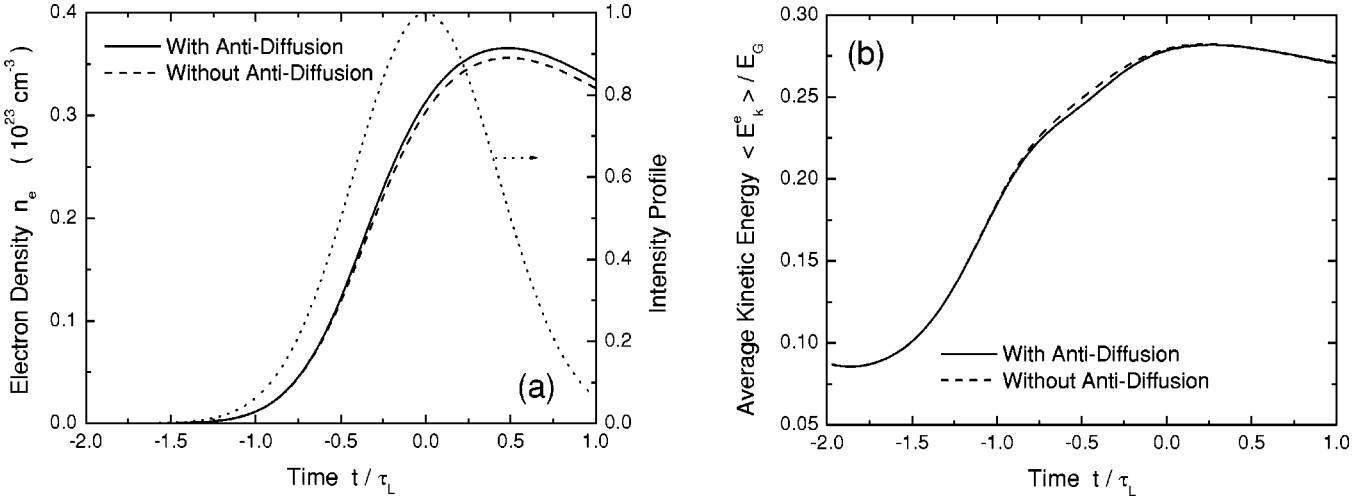

FIG. 6. Comparison of n_{3D}^e in (a) and $\langle E_k^e \rangle / E_G$ in (b) as a function of t/τ_L of a laser pulse by including (solid curves) or excluding (dashed curves) the antidiffusion current. For convenience, the intensity profile of an incident laser pulse is also shown in (a) by a dotted curve (right axis).

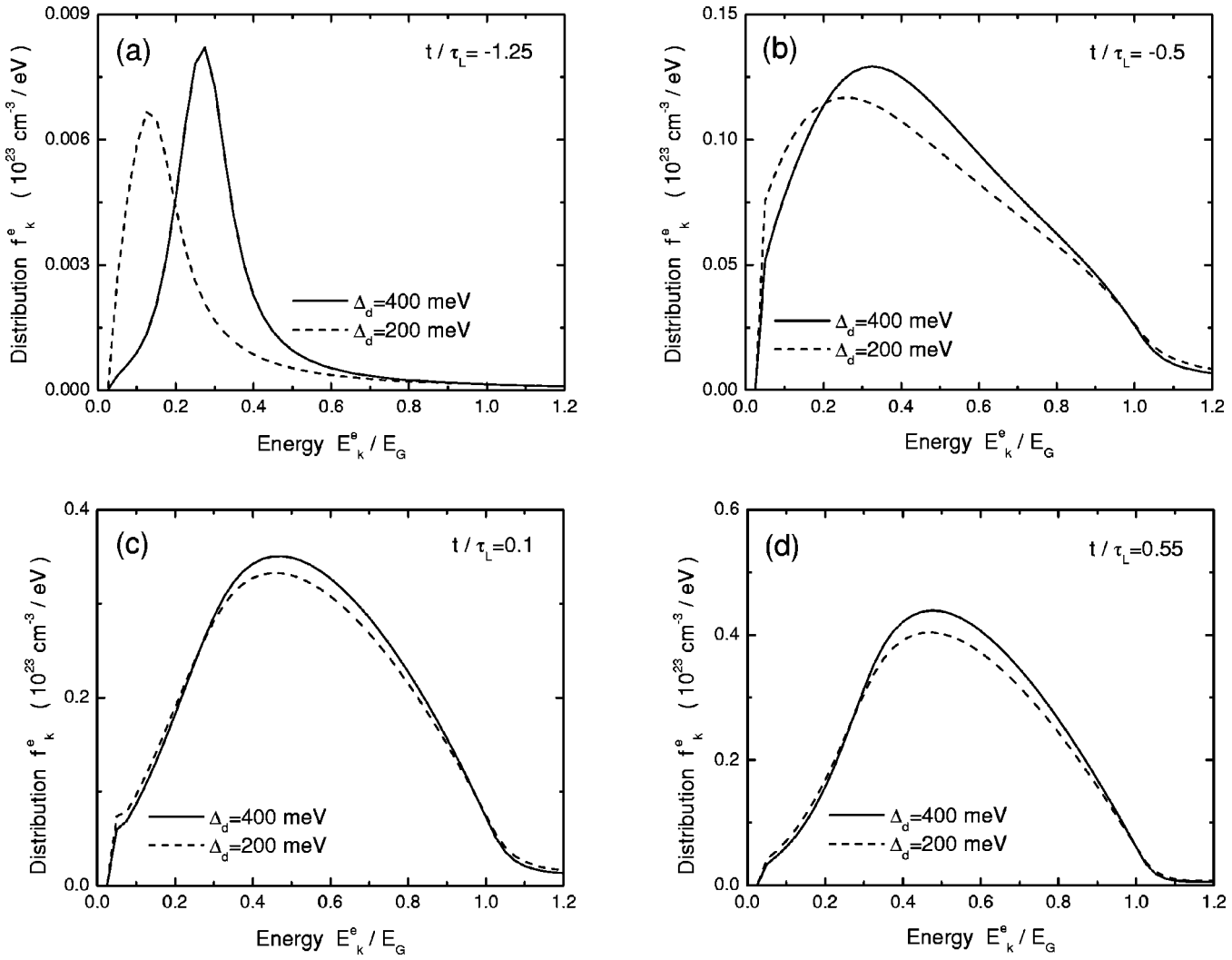

FIG. 7. Comparison of f_k^{e} as a function of $E_k^{\mathrm{e}}/E_{\mathrm{G}}$ at four different times with a larger (solid curves) or a smaller (dashed curves) laser-frequency detuning. The four times set in (a), (b), (c), and (d) are $t/\tau_{\mathrm{L}}=-1.25$, -0.5, 0.1, and 0.55, respectively.

trons at low energies is known to be due to spontaneous-phonon (thermal) emission. The electrons in high-energy states are found to be transferred to low-energy states through the emission of spontaneous phonons, shifting the peak down. Transferring electrons to the band edge enhances the upward antidiffusion process, producing a kinklike feature on the low-energy side of the peak. The accumulation of electrons around the edge further speeds up the Auger recombination process, leading to a smaller $n_{3\mathrm{D}}^{\mathrm{e}}$ after the peak intensity is reached.

Opposite to the energy loss of conduction electrons in the low-energy range, the energy gain of electrons in the whole energy range is through classical joule heating from power dissipation of the laser field within semiconductors. Joule heating has an opposite effect on f_k^{e} compared with that for thermal emission. In this case, the electrons in low-energy states are transferred to high-energy states by energy drift. This results in a shifting-up of the peak in f_k^{e}. Moreover, the impact ionization is enhanced by moving electrons up in energy space, which is reflected in the increase of $n_{3\mathrm{D}}^{\mathrm{e}}$ after the intensity peak is reached.

It is well known that single-photon absorption is a resonant process, which implies that a peak in f_k^{e} should occur initially at the energy determined by the laser-frequency detuning away from the band edge. We depict f_k^{e} as a function of $\tilde{E}$ at four different times of a laser pulse for two detunings $\Delta_{\mathrm{d}}=\hbar\Omega_{\mathrm{L}}-E_{\mathrm{G}}=400$ meV (solid curves) and $\Delta_{\mathrm{d}}=200$ meV (dashed curves) in Figs. 7(a), 7(b), 7(c), and 7(d). At an early time $\tilde{t}=-1.25$ in (a), the peak position of f_k^{e} is solely determined by Δ_{d}. However, the final peak position is eventually determined by the balance among the different kinds of diffusion, thermal emission, and classical joule heating effect, and the peak position becomes independent of Δ_{d} as shown in (c) and (d). As seen in (a), especially for large Δ_{d}, the initial lack of electron occupation near the band edge is rapidly compensated for by thermal emission and thermal and field-dependent diffusion as well as the speed-up of impact ionization in (c) and (d). The enhanced impact ionization for large Δ_{d} increases $n_{3\mathrm{D}}^{\mathrm{e}}$ in Fig. 8(a) after $\tilde{t}=0$. Moreover, the initial higher-energy peak in f_k^{e} increases $\langle E_k^{\mathrm{e}}\rangle$ in Fig. 8(b) when $\tilde{t}<-0.5$.

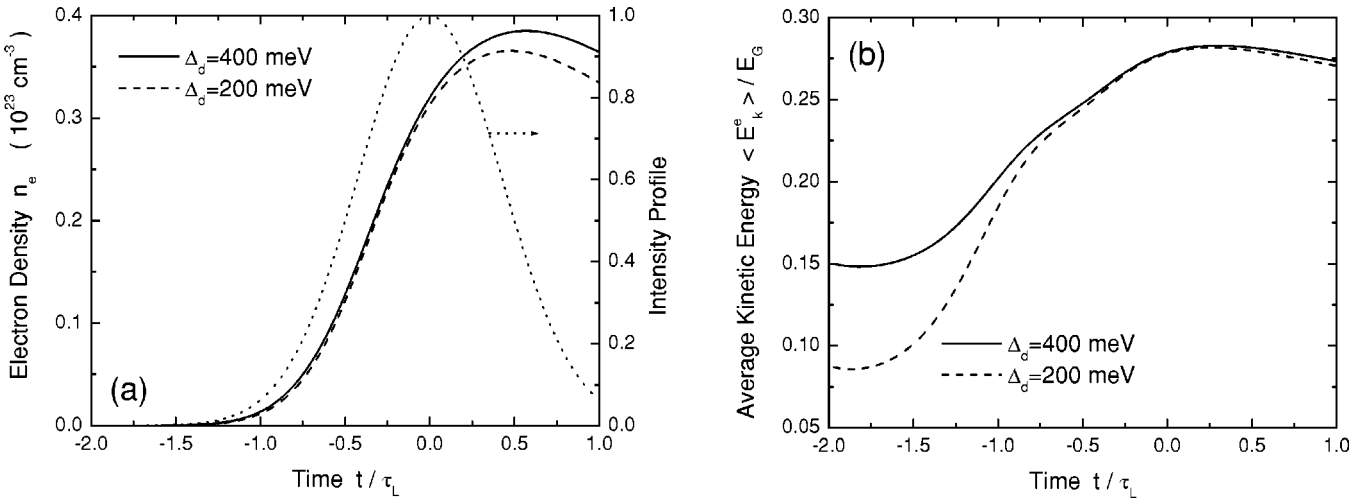

FIG. 8. Comparison of n^{e}_{3D} in (a) and $\langle E^{e}_{k}\rangle/E_{G}$ in (b) as a function of t/τ_{L} with a larger (solid curves) or a smaller (dashed curves) laser-frequency detuning. The intensity profile is also depicted in (a) by a dotted curve (right axis).

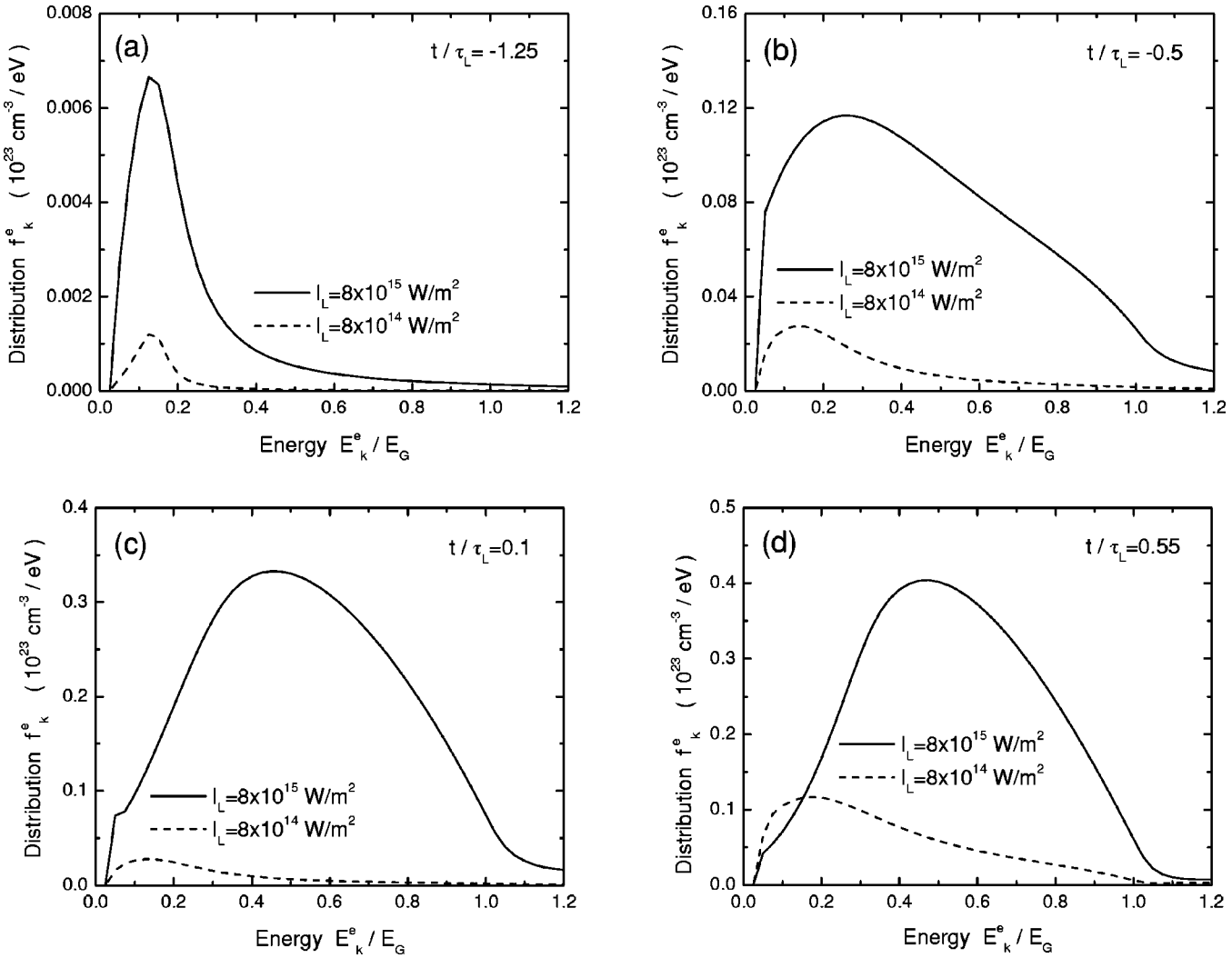

FIG. 9. Comparison of f^{e}_{k} as a function of E^{e}_{k}/E_{G} at four different times with a higher (solid curves) or a lower (dashed curves) laser intensity. The four times set in (a), (b), (c), and (d) are $t/\tau_{L}=-1.25$, -0.5, 0.1, and 0.55, respectively.

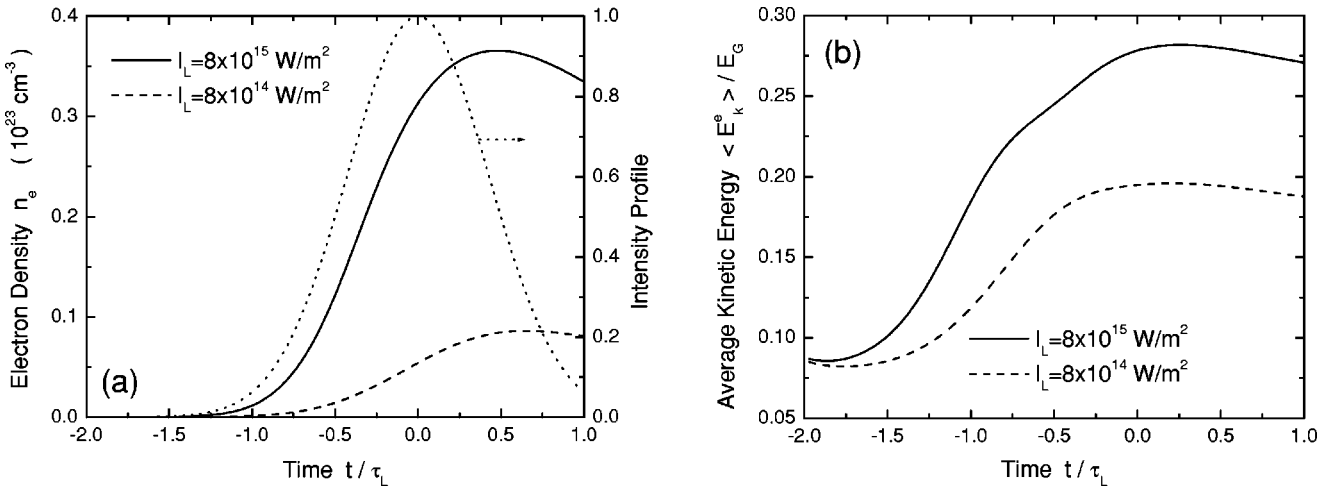

FIG. 10. Comparison of n^{e}_{3D} in (a) and $\langle E^{e}_{k}\rangle/E_G$ in (b) as a function of t/τ_L with a higher (solid curves) or a lower (dashed curves) laser intensity. The intensity profile is also displayed in (a) by a dotted curve (right axis).

Classical joule heating, field-dependent, and antidiffusion processes are all proportional to the intensity of the incident laser field. We find that these currents all play a crucial role in determining the internal dynamics of distributing electrons throughout the whole energy range. In Fig. 9 we demonstrate this effect by showing f^{e}_{k} as a function of $\tilde{E}$ at four different times relative to a laser pulse for two different peak intensities $I_L=8\times10^{15}$ W/m^2 (solid curves) and $I_L=8\times10^{14}$ W/m^2 (dashed curves). The magnitude of f^{e}_{k} becomes very large at high I_L because of the large optical absorption proportional to I_L. At $\tilde{t}=-1.25$ in (a), only the peak strength of f^{e}_{k} is greatly increased while its position is locked by Δ_d. The kinklike feature in (b), (c), and (d) becomes visible only for higher I_L due to the enhanced antidiffusion process. From (d) we find that the peak position at low I_L (dashed curve) is determined solely by Δ_d but at high I_L (solid curve) it is determined by a balance among the different kinds of diffusion, thermal emission, and classical joule heating since their contributions become important at high I_L. The increased absorption directly leads to a larger n^{e}_{3D} (solid curve) in Fig. 10(a), and the shifting-up of the peak in f^{e}_{k} (solid curve) results in a higher $\langle E^{e}_{k}\rangle$ in Fig. 10(b).

It is easy to understand that the lattice temperature T can affect the thermal emission and thermal diffusion. From our calculation, we find a spikelike feature at low T around the band edge due to the reduced thermal diffusion (imbalance between thermal diffusion and antidiffusion). At low T, E_G is increased compared to that at high T, which reduces the impact ionization. Moreover, the lack of electrons around the band edge due to reduced impact ionization suppresses the antidiffusion process and thus shifts up the peak of f^{e}_{k} and gives rise to a reduced peak strength. The suppression of the impact ionization directly contributes to a lower n^{e}_{3D}. On the other hand, the shifted-up peak produces a larger $\langle E^{e}_{k}\rangle$ after the laser intensity becomes strong.

VIII. CONCLUSION AND DISCUSSION

In conclusion, we have found a new antidiffusion contribution in the kinetic Fokker-Planck-type equation in the presence of a pulsed laser field as a correction to the spontaneous-phonon emission from drifting conduction electrons. Both classical joule heating and field-dependent diffusion are systematically derived instead of including them phenomenologically. The single-photon interband excitation, as well as the impact and Auger recombination resulting from the Coulomb scattering of two conduction electrons, have been included as the source terms up to second-order perturbation theory. We have also discussed some possible types of laser damage in semiconductors including optical, electrical, and structural damage.

Our numerical results have demonstrated a kinklike feature in the electron distribution function around the edge of the conduction band. The kink becomes appreciable at room temperature even when the laser field is not too strong. The energy spectra of the electron distribution function at different times relative to the time at which the peak of the laser pulse is reached have been used to explain the calculated transient behavior of the conduction-electron density and the average kinetic energy of electrons (electron temperature). The roles played by antidiffusion, laser-frequency detuning, laser intensity, impact ionization, Auger recombination, thermal diffusion, thermal emission, classical joule heating, lattice temperature, and sample mobility in determining the dynamics of the electron distribution in energy space have been analyzed and explained.

The validity of our current theory requires that (1) the maximum phonon energy be smaller than the average single-electron kinetic energy, (2) the electron-phonon interaction be weak, (3) the time period of the laser field be smaller than the relaxation time of conduction electrons, and (4) the phonon-assisted free-carrier absorption can be neglected for not too strong laser fields.

ACKNOWLEDGMENTS

One of the authors (T.A.) was supported by the National Research Council and wishes to thank Dr. Kenkre, Dr. Rudolph, and J. Jasapara for numerous very helpful discussions on the subject. We would also like to thank AHPCC where these calculations were carried out.

[1] B. C. Stuart *et al.*, Phys. Rev. Lett. **74**, 2248 (1995); Phys. Rev. B **53**, 1749 (1996).
[2] T. Kurosawa, J. Phys. Soc. Jpn. **20**, 937 (1965).
[3] L. H. Holway and D. W. Fradin, J. Appl. Phys. **45**, 677 (1974); **46**, 279 (1975).
[4] G. E. Uhlenbeck and L. S. Ornstein, Phys. Rev. **36**, 923 (1930).
[5] M. Sparks *et al.*, Phys. Rev. B **24**, 3519 (1981).
[6] M. V. Fischetti *et al.*, Phys. Rev. B **31**, 8124 (1985).
[7] G. Bastard, *Wave Mechanics Applied to Semiconductor Heterostructures* (Halsted Press, New York, 1988), p. 242.
[8] E. M. Epshtein, Sov. Phys. Solid State **11**, 2213 (1970).
[9] V. I. Mel'nikov, Pisma Zh. Éksp. Teor. Fiz. **9**, 204 (1969) [JETP Lett. **9**, 120 (1969)].
[10] An. V. Vinogradov, Zh. Eksp. Teor. Fiz. **68**, 1091 (1975).
[11] A. S. Epifanov, A. A. Manenkov, and A. M. Prokhorov, Zh. Éksp. Teor. Fiz. **70**, 728 (1975) [Sov. Phys. JETP **43**, 377 (1976)].
[12] B. G. Gorshkov *et al.*, Zh. Éksp. Teor. Fiz. **72**, 1171 (1977) [Sov. Phys. JETP **45**, 17 (1977)].
[13] A. Kaiser, B. Rethfeld, H. Vicanek, and G. Simon, Phys. Rev. B **61**, 11437 (2000).
[14] K. Flensberg, T. S. Jensen, and N. A. Mortensen, Phys. Rev. B **64**, 245308 (2001).
[15] T. Apostolova, D. H. Huang, P. M. Alsing, J. McIver, and D. A. Cardimona, Proc. SPIE **4679**, 124 (2002).
[16] D. H. Huang and D. A. Cardimona, Phys. Rev. A **64**, 013822 (2001).
[17] D. H. Huang and M. O. Manasreh, Phys. Rev. B **54**, 5620 (1996).
[18] C. Cohen-Tannoudji, B. Diu, and F. Laloë, *Quantum Mechanics*, (Wiley, New York, 1977), Vol. 2, p. 1283.
[19] G. D. Mahan, *Many-Particle Physics* (Plenum Press, New York, 1981), p. 38.
[20] D. H. Huang and S. K. Lyo, Phys. Rev. B **59**, 7600 (1999).
[21] T. Apostolova and Y. Hahn, J. Appl. Phys. **88**, 1024 (2000).
[22] N. A. Kroll and K. M. Watson, Phys. Rev. A **5**, 1883 (1972).